Experiments in Fluids 15, 385–392 (1993)

Experiments in Fluids

Optimal seeding for long pathlength multi-component laser Doppler anemometers

G. J. Brereton

Department of Mechanical Engineering and Applied Mechanics, The University of Michigan, Ann Arbor, MI 48109, USA

Received 31 January 1992 / Accepted: 26 April 1993

Abstract. There are optimal combinations of size and number density of seed particles which can maximize the processed data rate of laser Doppler anemometers (LDAs). When optical pathlengths are long, as in large scale water facilities, the choice and density of seeding particles determines the balance between the scattered-light intensity at a measuring volume and its extinction along the rest of the optical path, and so its intensity at a photodetector. These considerations must generally be coupled with knowledge of particle arrival statistics, detector performance, processor characteristics and signal conditioning to optimize data rate. However, in multi-component LDAs, coincidence requirements in data arrival times enforce a close approximation to a Poisson distribution in the processed data rate as a function of the number density of seed particles. This result leads to simple models for optimal number densities for seeding as a function of optical pathlength and related parameters.

1 Introduction

Laser-Doppler anemometry (LDA) has been employed predominantly for velocity measurement when the pathlength of laser light within the fluid is short and extinction of optical power is unimportant. However, when LDA is used as a non-intrusive instrument in large scale experimental facilities in which long optical pathlengths are unavoidable, attenuation within the optical medium can severely restrict the intensity of light scattered to photodetectors. This problem is compounded by the cost of high-power lasers necessary to offset losses through attenuation. If fiber optics are used for ease of movement of the optics relative to the laser and instrumentation, the power ratings of the fibers limit the permissible input power levels. These constraints require greater emphasis to be placed on the light scattering properties of seed particles, particularly if the LDA system is configured for backward scattering. Since the volume of seeding required for such facilities may be high and in situ experimentation is both time-consuming and expensive, it is useful to develop guidelines for optimal seeding which may be used in addition to the usual requirements that seed particles should be non-intrusive and faithfully follow the flow.

When LDA measurements are made to obtain turbulence statistics, it is important to acquire velocity data at acceptable rates, to resolve the contributions to these statistics from all relevant scales of motion in a reasonable period of time. In facilities such as tow tanks in which bodies are towed over finite distances, if data rates do not allow convergence of statistical quantities within a small number of traverses, the cost of experimentation can become prohibitively high. In the case of multi-component LDA, when joint statistics between different velocity components are desired, it is usually necessary to condition the validity of data processed by different channels of instrumentation on their arrival within a specified time interval in an effort to assure that the statistics describe single-point information. Since such conditioning reduces the rate at which valid data are recorded, the need to seed judiciously to maintain optimal data rates can become quite critical when using multi-component LDA over long optical pathlengths.

Surveys of literature on seeding practices for LDA typically reveal studies of particles and their scattering properties which produce acceptable results for applications involving short optical pathlengths (Durst et al. 1976). For example, the experiments of Adrian and Orloff (1977) reconcile particle visibility effects with computational results based on Mie scattering theory. Edwards (1987) has proposed definitions to clarify the various ways in which data rates may be reported, including a quantification of the processor-validated data rate with respect to the Taylor time microscale of the flow (Adrian 1983). The studies of Buchave (1979) and George (1979) have addressed the importance of particle arrival rates and their effects on bias when interpreted by burst processors. Recently, Brown (1989) carried out a computer simulation in which abnormally high bias errors reported in 3-component LDA systems were attributed to the beam geometry. However, little attention appears to have been given to the issue of how to select the size and number density of seed particles to optimize data rate, particularly when those

particles are also principal agents of extinction in optical systems. The criticality of this issue when using LDA for tow tank measurements motivated a combined theoretical and experimental study to deduce guidelines for optimal seeding in applications with long optical pathlengths.

2 Background

The rates at which validated multi-component data are recorded in LDA systems are dependent on many factors. They can include laser power, particle scattering properties, particle arrival rate at the measuring volume, detector sensitivity, processor speed and validation settings, and multi-channel coincidence requirements. While some of these factors may only be changed at great expense, the effects of using different particles, particle sizes, number densities, optical pathlengths and multi-channel coincidence requirements can be varied relatively easily and studied in controlled laboratory experiments. Their influence on processed data rate may be characterized by theoretical models which are described briefly below.

2.1 Particle size

The optimal size of particle for seeding with monosize particles in long pathlength LDA applications may be estimated from either geometric optics models or Mie-theory calculations, which model scattering by single spherical particles for the case of plane-wave illumination. If the irradiance of laser light entering the seeded medium is taken as I_0, its irradiance after propagation over distance z may be modeled as

$$I(z)=I_0 e^{-\int_0^z \alpha(z')dz'} \tag{1}$$

where α represents optical attenuation per unit length. In the absence of artificial seeding $\alpha(z)$ usually takes a constant value α_0. When seeding is present, it makes the additive contribution to α_0 of $\overline{N(z)Q_{ext}(d)\pi d^2}/4$ where $N(z)$ is the number density of seeding, d the particle diameter, and $Q_{ext}(d)$ the optical extinction efficiency, which may be determined from solutions of the Mie equations or taken as approximately 2 in the limiting case of large spherical particles (see, for example, Van de Hulst 1981). For an optical pathlength z between the entrance of laser light into the medium and its exit to the photodetector, the irradiance of particle-scattered light at the detector is modeled as

$$I(z)=I_0 V(d)Q_{sca}(d)\frac{\pi}{4}d^2 e^{-(\alpha_0 z+\int_0^z N(z')\overline{Q_{ext}(d)\pi d^2/4}\,dz')}. \tag{2}$$

In this expression, d is the individual particle diameter, $V(d)$ the particle visibility, and $Q_{sca}(d)$ represents the optical scattering efficiency of particles in the direction of the detector. Solutions of the Mie equations (Bohren and Huffman 1983) may be used to determine extinction and scattering properties of spherical particles as a function of their diameter and refractive index, as well as their visibility in intersecting beams (Adrian and Earley 1986). From the model, it may easily be shown that for a given uniform number density of monosize particles, the average intensity of scattered light received by the photodector may be maximized by choosing $\overline{d^2}=4/(NQ_{ext}\pi z)$. It is also apparent that the penalty for seeding with unnecessarily large particles at long pathlengths is excessive extinction, owing to domination of the exponential decay over the linear growth in irradiance as a function of particle cross-sectional area. The importance of this extinction effect may be demonstrated readily by Mie scattering computations of irradiance of backscattered light over pathlengths of the order of a few meters in water. For typical monosize particle seeding at $Nv=1$, suggested by a Poisson model for single-particle presence in the measuring volume v, the intensity of photodetected light can change by one or two orders of magnitude as the particle diameter is varied by as little as one micron. For this reason, a judicious choice of diameter of seeding particle can be critical to successful application of LDA over long optical pathlengths.

2.2 Particle arrival statistics

In steady incompressible flow which particles follow without lag, and for which particle convection is much more important than temporal diffusion, the presence of particles of statistically uniform distribution in a measuring volume may be modeled as a Poisson process. This process describes the probability of observing k different particles in a volume in time T as

$$Pr(k,\bar{\lambda}T)=\frac{(\bar{\lambda}T)^k}{k!}e^{-\bar{\lambda}T} \tag{3}$$

when the mean observation rate within the volume is $\bar{\lambda}$. It follows that the mean number of observed particles $\bar{k}$ is $\bar{\lambda}T$. Although unsteady (turbulent) flow can yield correlation between the momentary particle distribution and the instantaneous convection velocity, described by more general Mandel probability distributions (Erdmann and Gellert 1976), results presented later in this paper implied that this correlation effect might be unimportant in the turbulent flows under study. Thus the Poisson process was taken as the particle arrival model for determining strategies for optimal seeding.

2.3 Processed data rate model

The processed data rate depends upon the validation criteria of the processor, shift frequencies, thresholds, electronics gains, particle arrival rates and other factors. It

also depends on the photodetector output exceeding certain thresholds yet not saturating others and so is, in general, complex. However, when time coincidence in the detection of multi-channel data is used to improve the likelihood of obtaining single point statistics, it has the effect of validating data when a single particle is in the measuring volume. In this case, the single particle arrival rate may be modeled in direct proportion to

$$\langle\lambda\rangle Pr(k, \langle\lambda\rangle T) \quad \text{when} \quad k=1\,. \tag{4}$$

The processed data rate should then depend on the joint likelihoods of single particle presence in the measuring volume and of the light scattering capabilities of that particle providing a detectable signal. The latter condition may be expressed as

$$Pr\left(I_0 V(d) Q_{sca}(d) \frac{\pi}{4} d^2 e^{-(\alpha_0 z + \int_0^z N(z') \overline{Q_{ext}(d)\pi d^2/4}\, dz')} > J_{crit} \right) \tag{5}$$

where J_{crit} is the minimum optical energy per unit time necessary to provide a detectable signal above background noise for given instrumentation settings. Since seeding is described by a distribution in size, this condition leads to the notion of a critical value of the product of particle diameter, scattering efficiency, and visibility necessary to yield a detectable signal under given optical conditions and fixed electronic amplification. Thus

$$\left[V(d) Q_{sca}(d) \frac{\pi}{4} d^2 \right]_{crit} = \frac{J_{crit}}{I_0} e^{(\alpha_0 z + \int_0^z N(z') \overline{Q_{ext}(d)\pi d^2/4}\, dz')} \tag{6}$$

and the processed data rate may be modeled in direct proportion to

$$\langle\lambda\rangle Pr(k, \langle\lambda\rangle T)\, Pr(V(d)_{sca}(d) d^2 > [V(d) Q_{sca}(d) d^2]_{crit}) \quad \text{when} \quad k=1. \tag{7}$$

If reasonable assumptions may be made about the size distribution of seed particles, the validity of these models and the functional forms of the joint conditions which determine the processed data rate may be found with the help of experiments. In this study, the proposed model for the processed data rate was evaluated for a two-channel LDA system equipped with burst counters and operating at typical instrumentation settings for measurement of velocity in a turbulent flow.

3 Experimental methodology

A series of controlled experiments were carried out to establish the functional dependence of processed data rate on seeding parameters and optical pathlength. The experiments were designed to first check the premise that laser light was attenuated according to an exponential dependence on pathlength and then characterize the influence of different number densities and pathlengths on processed data rate, for different sizes and types of seed particle.

The experiments were carried out in a 10-gallon water tank within which an agitation pump, operating as a closed-loop system, sustained an unsteady turbulent three-dimensional flow at a Reynolds number (referenced to tank width) of 15,000. Various seeding particles (rutile titanium dioxide, silicon carbide, alumina) of different sizes were used for the experiments. Samples of the selected particles were examined under microscopes to check their approximate size against pre-determined values and so estimate their volumes. Knowing their specific gravities, the mass of each substance required to provide a desired number density in the 10 gallon system could be measured using a milligram scale. After weighing, particles were mixed with a small amount of water and a milli-molar solution of a surfactant (Triton X-100) to act as an anti-flocculant. They were then added in precise quantities to water in the tank to provide known number densities of seeding. The tank contained tap water supplied through a 1 μm filter. At all experimental conditions of this study, the data rate recorded from residual particles was at least an order of magnitude smaller than that achieved when samples of seed particles were first added (in increments of 3×10^8 m^{-3} in number density).

The LDA system was in a standard two-component 4-beam configuration with an argon ion laser, Dantec transmitting and receiving optics with a 310 mm front lens, and frequency shifting in both channels. The signal processors were Dantec 55L96a counters operated in fixed fringe mode (8 zero crossings, 5/8 proportional validation within 3% accuracy). Time coincidence in the arrival of validated date was enforced by digital circuitry in programmable logic arrays on each of two Dantec 92G31 transient burst recorder boards within a laboratory computer. The time-averaged data rate could then be deduced as the elapsed time necessary to record a prescribed number of valid data pairs. The LDA was operated as an on-axis backscatter system and positioned on a motored traverse, for ease of variation of the optical pathlength within the seeded medium. All experiments were carried out at the same laser power to eliminate the possibility of varying optical noise levels. Likewise, all electronic gains in counters and photodetectors were kept at constant values. In this way, the apparatus was used to make systematic measurements of the processed data rate as a function of optical pathlength, seed particle number density, and coincidence criteria for different seed particles.

4 Experimental results

The functional form for the joint conditions of the validated data rate model was explored by independent

assessments of: (i) the fidelity of the scattered light attenuation model; (ii) the dependence of validated data rate on particle presence in the measuring volume; and (iii) the dependence of validated data rate on the likelihood of scattered light exceeding an energy threshold at the detector. These separate effects were then combined within a general model for the processed data rate in long pathlength LDA systems at high seeding levels. Experimental determination of the model components is described below.

4.1 Evaluation of the attenuation model

For uniform seeding with a sample of particles of the same composition and size distribution, the attenuation model employed in (2) may be expressed as

$$\bar{I}(z) \propto I_0 e^{-(\alpha_0 z + N\overline{Q_{ext}(d)\pi d^2} z/4)}, \tag{8}$$

where $\bar{I}$ is the mean irradiance of transmitted light. With the input irradiance (laser power) held constant and the pathlength fixed, the exponential decay in irradiance with increasing number density was verified experimentally for number densities from 10^9 to 10^{13} m^{-3}. As a rough check on the value $\overline{d^2}$ used for sizing and evaluating the number density of the seed particle, the gradient of $\ln(\bar{I})$ with respect to N was compared with $Q_{ext}\pi\overline{d^2}z/4$. This comparison required the approximation that the coupled effects of diameter and scattering efficiency could be treated separately without changing the order of the estimate of $\overline{d^2}$. When Q_{ext} was taken as about 2, typical of many seeding particles in water, the discrepancy in this comparison was less than 5% for pre-sized particles such as nominally 1.5 μm spherical silicon carbide (TSI Model 10081). When the lognormal distribution used to size these particles was used to weight Mie-thoery calculations of $\overline{Q_{ext}(d)d^2}$, a comparable discrepancy with $\overline{Q_{ext}(d)}.\ \overline{d^2}$ was found. The exponential decay model was followed equally well by non-spherical particles such as rutile titanium dioxide.

4.2 Data-rate as a function of particle presence

The dependence of validated data rate on particle number density (and so the probability of particle presence in the measuring volume) was measured by varying N while keeping Nz (and so the attenuation factor in (8)) constant, for seeding with samples of particles of the same composition and size distribution. For the case of nominally 1.5 μm silicon carbide particles, the results are shown in Fig. 1, in which the abscissa is the dimensionless number density Nv. The measuring volume was estimated by translating a 2-mil (50 μm) wire through the beam intersection region by micrometer and assessing the dimensions along the principal axes for which validated signals

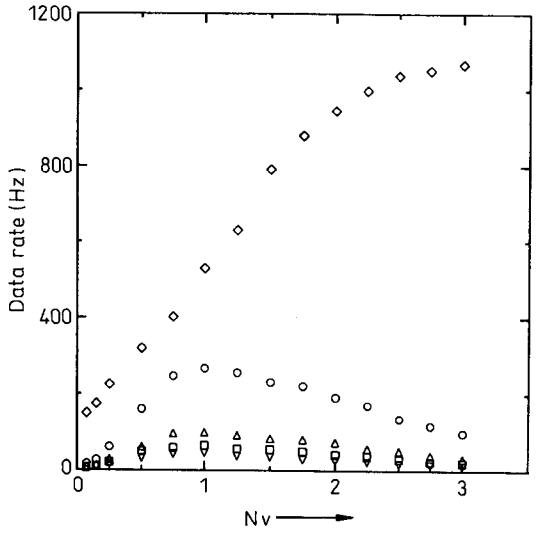

Fig. 1. Dependence of processed data rate on number density N for constant Nz, thereby maintaining constant irradiance at the photodetector and measuring volume; ○, $T_{coinc}/T_{conv}=0.5$; △, $T_{coinc}/T_{conv}=0.05$; □, $T_{coinc}/T_{conv}=0.025$; ▽, $T_{coinc}/T_{conv}=0.0125$; ◇, no coincidence requirement. Seeding is with silicon carbide particles of nominal diameter 1.5 μm

were recorded in both channels. For the instrumentation settings of this study, v was approximately one third of the $1/e^2$ volume. Means and variances of the velocities measured in each channel exhibited negligible dependence on the choice of coincidence time.

When a single channel of instrumentation was employed, with no conditioning (apart from the 5/8 validation of the counter and an inability to count during the two clock cycles after each validated measurement), the processed data rate increased monotonically for values of Nv as high as 3, with some flattening off when more than two particles, on average, were in the "two-channel" measuring volume (which was about one-third the size of the "single-channel" measuring volume). The effect of requiring coincidence in data arrival times in two channels was to cause the data to peak at approximately one particle per measuring volume. This result is consistent with the idealized case of Poisson particle-arrival statistics and a measurement instrument which only validates data when a single particle scatters light within the measuring volume. The different coincidence time intervals (T_{coinc}) employed for these tests are expressed as fractions of the average time a particle would spend in the measuring volume when convected through it by the mean flow (T_{conv}). The coincidence conditioned data of this figure are plotted in Fig. 2 after normalization by a constant multiple (e^{-1}) of each peak data rate, together with a curve describing the Poisson distribution for a single particle in the measuring volume, approximated as:

$$\bar{\lambda} T e^{-\bar{\lambda}T} = Nv e^{-Nv}. \tag{9}$$

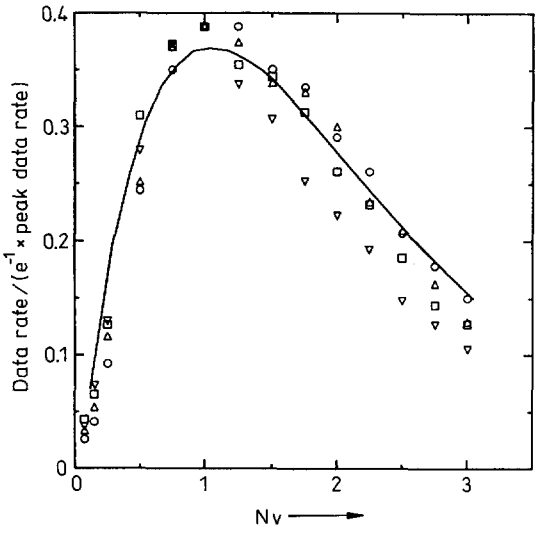

Fig. 2. Normalized dependence of processed data rate on number density for constant Nz; ○, $T_{coinc}/T_{conv}=0.5$; △, $T_{coinc}/T_{conv}=0.05$; □, $T_{coinc}/T_{conv}=0.025$; ▽, $T_{coinc}/T_{conv}=0.0125$; ———, single particle Poisson distribution

It is clear from this figure that the effect of conditioning data validity on a coincidence requirement is to enforce a close approximation to a Poisson distribution in the *processed* data rate, as a function of particle number density. Comparable results were obtained for rutile titanium dioxide and alumina particles, though the statistical convergence of these data was somewhat slower owing to the broader size distributions of these samples.

These results imply that the use of a coincidence requirement with multi-channel data restricts valid signals to those received when there is a single particle in the measuring volume common to both channels, and that particle arrival is well modeled as a Poisson process. The greater data rates achieved for single channel operation are due, in part, to the greater size of measuring volume and the lenience with which a single processor validates signals from multiple particles in the measuring volume. Other plausible explanations, in terms of operation of coincidence circuitry and on counter logic, might be explored using simulations of the kind described by Brown (1989).

4.3 Dependence of data rate on a scattered-light intensity threshold

The dependence of validated data rate on the likelihood of the light scattered to the photodetector exceeding a threshold was examined by measuring the processed data rate as a function of optical pathlength z. The number density and the measuring volume were unchanged so that the single particle arrival rate, modeled in proportion of $Nv\,e^{-Nv}$, remained constant. The mean components of velocity in the turbulent flow were comparable at all transverse positions so that the effect of varying z would scarcely affect parameters other than the optical pathlength. For seeding with nominally 1.5 μm silicon carbide particles, the dependence of processed data rate on z (expressed as the dimensionless pathlength $N\overline{Q_{ext}}\pi d^2 z/4$) is shown in Fig. 3 for various coincidence times. The decay in processed data rate with increasing optical pathlength follows a close approximation to an exponential decay of approximately one decade over 1.6 dimensionless pathlengths, and bears no relation to the abrupt roll-off expected for strictly monosize particles at a critical pathlength. Comparable results were obtained for seeding with other particles used in this study.

Since the single-particle arrival rate was fixed in this series of experiments, the validity of the joint probability model of (7) then depends on whether

$$Pr(V(d)Q_{sca}(d)d^2 > [V(d)Q_{sca}(d)d^2]_{crit}) \qquad (10)$$

follows an exponential decay with increasing optical pathlength z. This dependence may be demonstrated for spherical particles by computing $V(d)$ and $Q_{sca}(d)$ from Mie theory, following the procedure of Adrian and Earley (1986), to evaluate the product $V(d)Q_{sca}(d)\,d^2$ as a function of d. While this function typically varies erratically over small changes in d, it remains bounded. By using the lognormal distribution (with which the test particles were sized) and integrating with respect to $V(d)Q_{sca}(d)d^2$, evaluation of the probability function of (10) may be completed numerically. For the case of on-axis backscatter for a range of plausible beam-intersection angles, with

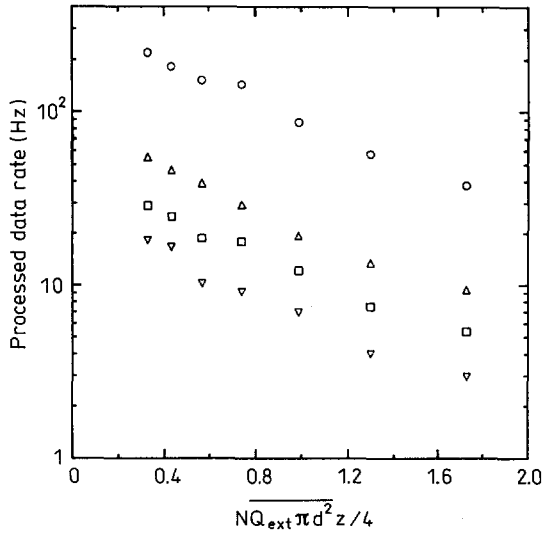

Fig. 3. Variation of recorded data rate with optical pathlength z for seeding at constant number density; ○ $T_{coinc}/T_{conv}=0.5$; △, $T_{coinc}/T_{conv}=0.05$; □, $T_{coinc}/T_{conv}=0.025$; ▽, $T_{coinc}/T_{conv}=0.0125$. Seeding is with silicon carbide particles of nominal diameter 1.5 μm with $N=4.3\times10^{11}$ m^{-3}

a circular collection aperture just within the laser beams, this probability function is shown in Fig. 4. The complex variations of visibility and scattering coefficients with d give the appearance of scatter about an otherwise smooth probability function, which is enforced by the weighting of the distribution within an integral expression.

It is clear from Fig. 4 that the probability of the intensity of scattered light exceeding a given threshold is well described by the exponential model:

$$Pr(VQ_{sca}d^2 > [VQ_{sca}d^2]_{crit}) \simeq e^{-\text{const.}[V(d)Q_{sca}(d)d^2]_{crit}} \quad (11)$$

for probabilities as low as 0.2, which corresponded to roughly all but the largest 6% of the particles in this distribution. Comparable results were obtained for other distributions of particle size (i.e. the Rosin-Rammler model generalized by Lefebvre (1989)) in the 1–10 micron range typically used for seeding. From (6), for uniform seeding along the optical pathlength,

$$[V(d)Q_{sca}(d)d^2]_{crit} \propto e^{\alpha_0 z + N\overline{Q_{ext}(d)\pi d^2}z/4} . \quad (12)$$

When $\alpha_0 z + N\overline{Q_{ext}(d)\pi d^2}z/4 \lesssim 0.3$, as is usually the case even for heavily seeded long-range LDA systems,

$$[V(d)Q_{sca}(d)d^2]_{crit} \propto 1 + \alpha_0 z + N\overline{Q_{ext}(d)\pi d^2}z/4 \quad (13)$$

in which case

$$Pr(VQ_{sca}d^2 > [VQ_{sca}d^2]_{crit}) \simeq e^{-\text{const.}(1+\alpha_0 z + N\overline{Q_{ext}\pi d^2}z/4)} \quad (14)$$

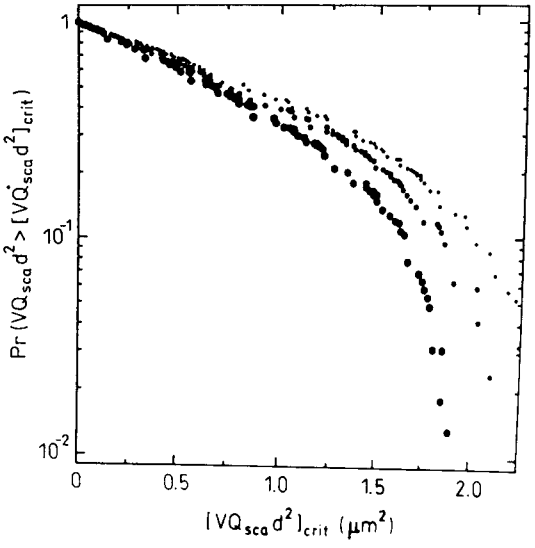

Fig. 4. Mie-theory calculations of the probability of $V(d)Q_{sca}(d)d^2$ exceeding threshold values, for a lognormal distribution of silicon carbide particles of mean diameter 1.5 μm, geometric standard deviation 1.4. Calculations are for the green line of an argon-ion laser in water, with beam intersection half-angles •, $\kappa = 4°$; •, $\kappa = 6°$; ●, $\kappa = 8°$

which recovers the exponential decay with increasing optical pathlength.

For long optical pathlengths in well seeded liquids, α_0 may be neglected so that a convenient model for $Pr(VQ_{sca}d^2 > [VQ_{sca}d^2]_{crit})$ is a constant multiple of $e^{-\beta N\overline{Q_{ext}(d)\pi\frac{d^2}{4}}z}$ where β is a coefficient of order one which incorporates average effects of refractive index, visibility and scattering efficiencies over the distribution in particle size. For the data of Fig. 3, and a decay of one decade over 1.6 dimensionless pathlengths, β took the value 1.4.

4.4 Comparisons of the data rate model with measurements

The multiplicative combination of the models for single particle arrival rate and for data rate dependence on scattered light intensity yields an expression proportional to the processed data rate, of the form: $\langle\lambda\rangle Pr(k, \langle\lambda\rangle T)$ $Pr(VQ_{sca}d^2 > [VQ_{sca}d^2]_{crit})$ for $k = 1$. When $\langle\lambda\rangle T$ is approximated as Nv, and the local exponential approximation for scattered light exceeding an intensity threshold is used, the processed data rate may be expressed as a constant multiple of:

$$Nve^{-Nv}e^{-\beta N\overline{Q_{ext}\pi d^2}z/4} . \quad (15)$$

If the dependence of processed data rate on N is investigated at fixed z, it is convenient to define a new effective volume $C = v + \beta\overline{Q_{ext}\pi d^2}z/4$. Thus the processed data rate is the same constant multiple of $(v/C)NCe^{-NC}$. For fixed pathlength z and fixed particle size/composition, C and v are constant so measurements of the processed data rate for varying N should follow a single event Poisson distribution, peaking at $NC = 1$. Experimental data for variation of processed data rate with N at fixed z are shown in Fig. 5, with Nv as the abscissa. It is clear that peak data rates are achieved for values of Nv lower than one when coincidence conditioning of data is enforced. The data of Fig. 5 may also be plotted as a function of NC and are shown, after normalization by their peak data rate (and scaled by e^{-1}), in Fig. 6. When plotted in these normalized forms there is good agreement with the Poisson curve because the number densities corresponding to $Nv = 1$ in Fig. 5 and $NC = 1$ in Fig. 6 are almost exactly in proportion to $v/(v + \beta\overline{Q_{ext}\pi d^2}/4z)$. The scaling of the curves in Fig. 5 for different coincidence time intervals is also almost identical to that of Fig. 1. These results provide experimental support for the validity of the proposed processed data rate model. The range of seeding levels over which it has been tested corresponds to $N\overline{Q_{ext}\pi\frac{d^2}{4}}z$ of orders 0.1 to 1, for silicon carbide, titanium dioxide and alumina seed in the 1–10 micron range. For broader ranges of seeding densities, models for $Pr(VQ_{sca}d^2 > [VQ_{sca}d^2]_{crit})$ based on more sophisticated size distributions may be employed and tested in the same way.

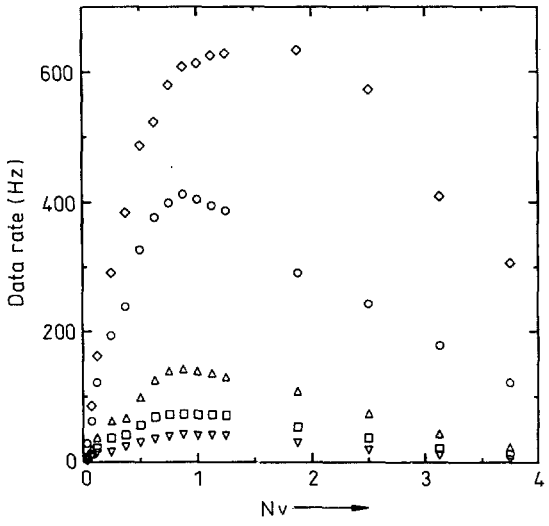

Fig. 5. Dependece of processed data rate on number density over a constant optical pathlength; ○, $T_{coinc}/T_{conv}=0.5$; △, $T_{coinc}/T_{conv}=0.05$; □, $T_{coinc}/T_{conv}=0.025$; ▽, $T_{coinc}/T_{conv}=0.0125$; ◇, no coincidence requirement. Seeding is with silicon carbide particles of nominal diameter 1.5 μm

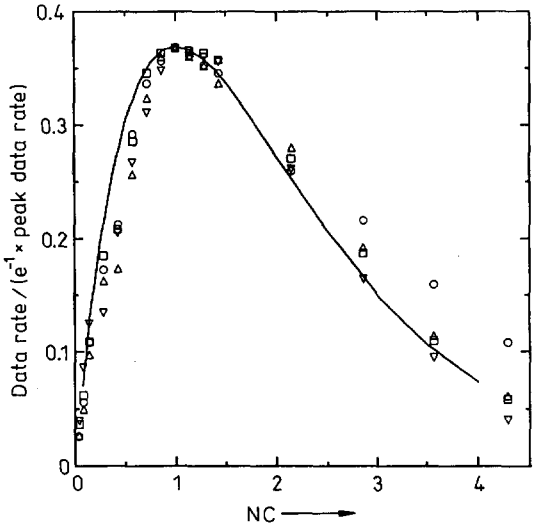

Fig. 6. Normalized dependence of processed data rate on number density-effective volume product over a constant optical pathlength; ○, $T_{coinc}/T_{conv}=0.5$; △, $T_{coinc}/T_{conv}=0.05$; □, $T_{coinc}/T_{conv}=0.025$; ▽, $T_{coinc}/T_{conv}=0.0125$; ———, single particle Poisson distribution

5 Guidelines

For multi-component LDAs which use coincidence requirements for data validation, the processed data rate appears to be well represented as a multiple of the product $\langle\lambda\rangle Pr(k, \langle\lambda\rangle T)\, Pr(VQ_{sca}d^2 > [VQ_{sca}d^2]_{crit})$ when $k=1$. Modeling the single particle arrival rate as a Poisson process leads to re-expression of the processed data rate as a constant (dependent on, amongst other factors, the coincidence window employed) multiplied by:

$$Nv\, e^{-Nv}\, Pr(VQ_{sca}d^2 > [VQ_{sca}d^2]_{crit}). \tag{16}$$

For fixed laser power and photodetection gain, differentiation with respect to N yields a maximum processed data rate at the optimal seeding level:

$$Nv_{opt} = \frac{1}{1 - \dfrac{1}{vPr(VQ_{sca}d^2 > [VQ_{sca}d^2]_{crit}} \dfrac{d}{dN} [Pr(VQ_{sca}d^2 > [VQ_{sca}d^2]_{crit})]}. \tag{17}$$

For a given seed, and maximum available laser power and photodetector amplification, (17) guides the optimal density of seeding. If the model $Pr(VQ_{sca}d^2 > [VQ_{sca}d^2]_{crit}) \propto e^{-\beta N \overline{Q_{ext}\pi d^2} z/4}$ is used, for a given seed and optical configuration, the maximum processed data rate is obtained for the number density-volume product:

$$Nv_{opt} = \frac{1}{1+\beta \overline{Q_{ext}\pi d^2}\, z/(4v)}. \tag{18}$$

Equation (18) guides the value of N which should be chosen to maximise processed data rate. In the case of short optical pathlengths, it correctly simplifies to $Nv \simeq 1$ which is well-known as a guideline for seeding, based on single-particle Poisson arrival statistics. For a given size of measuring volume, the optimal seeding density is reduced below its short-pathlength value by effects of extinction such as increased particle cross-sectional area and greater extinction coefficients. In practical applications in which long focal-length lenses are employed, beam expansion and/or pinholes are used to reduce v, and moderate sizes of seeding particle are used, values of Nv_{opt} of the order of 0.1 will frequently maximize the processed data rate.

It is possible to extend these guidelines for processed data rate to media in which there are already residual light scattering particles, as is often the case in large-scale water facilities and in particulate flows. If the residual and seed particles are denoted by the subscripts r and s respectively, the probability of detection of a single scattering particle in the measuring volume is $Pr(1)_r\, Pr(0)_s + Pr(0)_r\, Pr(1)_s$. For each component i of the particle mixture, $Pr(1)_i$ may be modeled as $N_i v\, e^{-N_i v}\, Pr(VQ_{sca}d^2|_i > [VQ_{sca}d^2]_{i,crit})$. The probability of no detection of a component, $Pr(0)_i$, may be expressed as $e^{-N_i v} + N_i v\, e^{-N_i v}\, Pr(VQ_{sca}d^2]_i > [VQ_{sca}d^2]_{i,crit}) + \cdots$ or, if summed as a geometric progression, $e^{-N_i v}/(1 - N_i v\, Pr(VQ_{sca}d^2|_i <$

$[VQ_{sca}d^2]_{i,crit}$)). The modeled probability may be differentiated with respect to the number density of seed particles to yield the value of $N_s v$ which corresponds to the maximum processed data rate.

As an example, consider the case of strong illumination or photodetection at very high gains when the product $N_i v\ Pr(VQ_{sca}d^2|_i < [VQ_{sca}d^2]_{i,crit})$ tends to zero. If $Pr(VQ_{sca}d^2|_i > [VQ_{sca}d^2]_{i,crit})$ is modeled as exponentially dependent on z, the processed data rate will be maximized when

$$N_s v_{opt} = \frac{1}{1+\beta_s \overline{Q_{ext_s}} \pi \overline{d_s^2} z/(4v)} - N_r v \left(\frac{1+\beta_r \overline{Q_{ext_s}} \pi \overline{d_s^2} z/(4v)}{1+\beta_s \overline{Q_{ext_s}} \pi \overline{d_s^2} z/(4v)} \right) \frac{e^{-\beta_r (N_r \overline{Q_{ext_r}} \pi \overline{d_r^2} z/4 + N_s \overline{Q_{ext_s}} \pi \overline{d_s^2} z/4)}}{e^{-\beta_s (N_r \overline{Q_{ext_r}} \pi \overline{d_r^2} z/4 + N_s \overline{Q_{ext_s}} \pi \overline{d_s^2} z/4)}}, \quad (19)$$

which further reduces the seed number density-measuring volume product below its value in an uncontaminated system. It can easily be shown that, for this model of residual light scattering particles and purposefully added seeding, the addition of *any* seeding will serve only to reduce the processed data rate when the number density-measuring volume product of residual light scattering particles attains the level:

$$N_r v_{opt} = \frac{1}{1+\beta_r \overline{Q_{ext_r}} \pi \overline{d_r^2} z/(4v)} \frac{e^{-\beta_r (N_r \overline{Q_{ext_r}} \pi \overline{d_r^2} z/4 + N_s \overline{Q_{ext_s}} \pi \overline{d_s^2} z/4)}}{e^{-\beta_s (N_r \overline{Q_{ext_r}} \pi \overline{d_r^2} z/4 + N_s \overline{Q_{ext_s}} \pi \overline{d_s^2} z/4)}}. \quad (20)$$

For greater residual seeding levels, dilution is necessary to improve data rates. Thus (20) provides a meaningful way of assessing when facility water contamination has become excessive and cleaning is necessary. Similar results may be obtained for particle size distributions modeled by Rosin-Rammler or related fits, though the algebra is more tedious and numerical evaluation may be more appropriate.

These guidelines, and other straightforward extensions to systems with more complex mixtures of seedings, are useful if reasonable estimations can be made of the average diameter and number density of residual light scattering particles, and of their size distributions. While the product $N_r \overline{d_r^2}$ may be obtained from simple measurements of the attenuation of light through a sample of the facility water, the additional information necessary to make use of these results typically requires particle sizing equipment to estimate a mean residual particle diameter, together with assumptions of sphericity, knowledge of refractive indices and familiarity with Mie theory computations. Nonetheless, these guidelines show how considerable improvements may be made over seeding with existing ones and should prove useful for researchers who undertake LDA measurements over long pathlengths in water facilities.

Acknowledgements

This study was carried out under the support of the University Research Initiative of the Office of Naval Research (Contract N00184-86-K-0684). The improvements suggested by Prof. D. T. Walker, Prof. R. J. Adrian and an anonymous reviewer are gratefully acknowledged, as is the diligence of Dr. J.-L. Hwang in programming, testing and debugging the time-coincidence data acquisition software.

References

Adrian, R. J. 1983: Laser velocimetry. In: Fluid Mechanics Measurements (Ed. Goldstein, R. J.), New York: Hemisphere pp. 155–244.

Adrian, R. J.; Orloff, K. L. 1977: Laser anemometer signals: visibility characteristics and application to particle sizing. Appl. Opt. 16, 677–684

Adrian, R. J.; Earley, W. I. 1986: Evaluation of laser-Doppler velocimeter performance using Mie scattering theory. Rpt. No. 479, Dept. of Theoretical and Applied Mechanics, University of Illinois, Urbana-Champaign

Bohren, C. F.; Huffman, D. R. 1983: Absorption and scattering of light by small particles New York: Wiley

Brown, J. L. 1989: Geometric bias and time coincidence in 3-dimensional laser Doppler velocimeter systems. Exp. Fluids 7, 25–32

Buchave, P. 1979: The measurement of turbulence with the burst-type laser-Doppler anemometer-errors and correction methods. Technical Report No. TRL-106, Turbulence Research Laboratory, SUNY, Buffalo

Durst, F.; Melling A.; Whitelaw J. H. 1976: Principles and practice of laser-Doppler anemometry. London: Academic Press

Edwards, R. V. 1987: Report of the special panel on statistical particle bias problems in laser anemometry. J. Fluids Eng. 109, 89–93

Erdmann, J. C.; Gellert, R. I. 1976: Particle arrival statistics in laser anemometry of turbulent flow. Appl. Phys. Lett. 29, 408–411

George, W. K. 1979: Processing of random signals. In: Proc. of the Dynamic Flow Conf. Skovlunde, Denmark

Lefebvre, A. H. 1989: Atomization and sprays. New York: Hemisphere

Van de Hulst, H. C. 1981: Light scattering by small particles. New York: Dover